

THE LUMINOSITY FUNCTION OF VOID GALAXIES IN THE SLOAN DIGITAL SKY SURVEY

FIONA HOYLE,¹ RANDALL R. ROJAS,¹ MICHAEL S. VOGLEY,¹ AND JON BRINKMANN²

Received 2003 September 26; accepted 2004 October 30

ABSTRACT

We measure the r -band luminosity function (LF) of a sample of 10^3 void galaxies over a large range of magnitude, $-21.5 < M_r < -14.5$. These objects were identified by Rojas et al. from the Sloan Digital Sky Survey as residing in regions with local galaxy density $\delta\rho/\rho < -0.6$ on a scale of $7 h^{-1}$ Mpc. We compare the void galaxy LF with that of galaxies in denser regions (so-called “wall” galaxies). The void galaxy LF is well fitted by a Schechter function with normalization $\Phi^* = (0.19 \pm 0.04) \times 10^{-2} h^3 \text{ Mpc}^{-3}$, characteristic magnitude $M_r^* - 5 \log h = -19.74 \pm 0.11$, and faint-end slope $\alpha = -1.18 \pm 0.13$. A comparable measurement of the LF of wall galaxies yields $\Phi^* = (1.42 \pm 0.03) \times 10^{-2} h^3 \text{ Mpc}^{-3}$, $M_r^* - 5 \log h = -20.62 \pm 0.08$, and $\alpha = -1.19 \pm 0.07$. Thus, we find that void galaxies are characteristically fainter than wall galaxies, but we do not find a significant dependence of the slope of the LF at the faint end on environment alone. The latter result suggests that there is no excess of dwarfs in voids, in contrast to predictions of cold dark matter (CDM) models. We split both the void and wall samples in half by density and find that the LFs of both the higher and lower density void galaxies and the lower density wall galaxies are similar in shape. However, the LF of wall galaxies in the highest density regions has a shallower faint-end slope, i.e., there are relatively fewer faint galaxies in the highest density regions. The LF of void galaxies is most similar to that of late-type galaxies in denser regions. The LFs of subsamples of wall galaxies that have blue $g - r$ color, spiral-like surface brightness profiles (Sérsic index $n < 2$), or relatively high star formation rates [$\text{EW}(\text{H}\alpha) > 5 \text{ \AA}$], have brighter M_r^* but faint-end slopes similar to those of void galaxies. In contrast, the LFs of wall galaxies with red $g - r$ color, elliptical-like profiles, or low star formation rates have significantly shallower faint-end slopes and brighter values of M_r^* than we find for void galaxies. We conclude that the void galaxy population is dominated by faint, late-type galaxies. The shift in M^* between the void and wall galaxy LFs is consistent with the shift of the mass function in voids predicted by extended Press-Schechter theory.

Subject headings: cosmology: observations — galaxies: distances and redshifts — large-scale structure of universe — methods: statistical

1. INTRODUCTION

One of the most fundamental properties of a distribution of galaxies is the distribution of their luminosities, known as the luminosity function (LF), $\Phi(L) = dN/dLdV$. Measurements of the galaxy LF have significantly improved in recent years as a result of both the increase in the size of galaxy redshift surveys and the use of large-format CCD cameras. The large solid angle and depth of the Two-Degree Field Galaxy Redshift Survey (2dFGRS) and the Sloan Digital Sky Survey (SDSS) allow highly accurate measurements of the local LF; Norberg et al. (2002b) measure the b_r -band LF from a sample of 110,500 galaxies from the 2dFGRS, and Blanton et al. (2003b) measure the r -band LF from a sample of over 140,000 galaxies from the SDSS.

These new samples of galaxies make it possible to study the dependence of the LF and other statistical measures on a large number of photometric and spectroscopic galaxy properties. Using the 2dFGRS data, Madgwick et al. (2002) measure the LF as a function of spectral type, Norberg et al. (2002a) study the dependence of galaxy clustering strength on luminosity, and Lewis et al. (2002) examine the environmental dependence of galaxy star formation rates. From SDSS galaxy redshift samples, Nakamura et al. (2003) study the LF as a function of galaxy morphology, Hogg et al. (2002, 2003) measure the overdensities of galaxy environments as a function of luminosity and color,

Gómez et al. (2003) probe galaxy star formation as a function of environment, Goto et al. (2003) examine the environment of passive spiral galaxies, and Balogh et al. (2004) look at the dependence of galaxy properties on luminosity and environment. These results consistently reveal strong trends with environment of the luminosity, morphology, star formation rate, and clustering of galaxies; galaxies in higher density regions tend to be redder, of earlier type, have lower star formation rates, and to be more strongly clustered. Some of these trends might be expected from the well-known morphology-density relation (Dressler 1980; Postman & Geller 1984). Less clear is whether, or how far, these trends extend to the other extreme, in the rarefied environments of voids.

In this paper, we focus on the LF of galaxies found in extremely underdense environments (i.e., galaxies in regions with $\delta\rho/\rho < -0.6$ measured on a scale of $7 h^{-1}$ Mpc). We refer to these as void galaxies. This study complements other LF analyses that have focused on galaxies found in different environments (see de Lapparent [2003] for a recent comprehensive review of LF measurements). Most previous analyses have focused on the LF of galaxies found in regions with densities equal to or higher than the density around field galaxies (e.g., Loveday et al. 1992; Marzke et al. 1994a, 1994b; Zucca et al. 1997; Ratcliffe et al. 1998; Lin et al. 1996; Folkes et al. 1999; Blanton et al. 2001, 2003b, 2005; Norberg et al. 2002b) or on galaxies in much higher density environments, such as clusters (see, e.g., Dressler 1978; Luggner 1986; Colless 1989; Gaidos 1997; Lumsden et al. 1997; Valotto et al. 1997; Rauzy et al. 1998; Garilli et al. 1999; Paolillo et al. 2001; Goto et al. 2002; Trentham & Hodgkin 2002; Trentham & Tully 2002; de Propris

¹ Department of Physics, Drexel University, 3141 Chestnut Street, Philadelphia, PA 19104; fiona.hoyle@drexel.edu, rrojas@mercury.physics.drexel.edu, vogeley@drexel.edu.

² Apache Point Observatory, P.O. Box 59, Sunspot, NM 88349-0059.

et al. 2003). Early studies of void galaxies probed their spectral and photometric properties (Moody et al. 1987; Weistrop et al. 1995; Popescu et al. 1997) and $H\text{I}$ content (Szomoru et al. 1996; Huchtmeier et al. 1997), but these samples were too small to allow measurement of the LF. Using the Center for Astrophysics Redshift Survey (CfARS; Geller & Huchra 1989), Grogin & Geller (1999) first measured the void galaxy LF for 46 galaxies in regions with density less than half of the mean density (i.e., $\delta\rho/\rho < -0.5$). Here we examine the LF of a sample of 10^3 void galaxies at somewhat lower density.

The LF of void galaxies provides a critical test of models for galaxy formation. CDM models predict the existence of many low-mass halos in voids (Dekel & Silk 1986; Hoffman et al. 1992). If these halos contain dwarf galaxies, then the void galaxy LF should have a steep faint-end slope. Including the effects of photoionization in theoretical models has been shown to restrict galaxy formation, which leads to a LF with a flatter faint-end slope (Benson et al. 2003b). Thus, measurement of the shape of the LF in voids is a key input to these models. More generally, the variation with environment of the galaxy LF is an important constraint on models that relate galaxy properties to halo masses (e.g., Berlind & Weinberg 2002).

To date, the observational situation is not clear. Surveys of dwarf galaxies indicate that they trace the same overall structures as “normal” galaxies (e.g., Bingelli 1989), and pointed observations toward void regions have failed to detect a significant population of faint galaxies (Kuhn et al. 1997; Popescu et al. 1997). However, Grogin & Geller (1999) found that the LF of void galaxies is quite steep at the faint end; the best-fit Schechter function has a faint-end slope $\alpha = -1.4 \pm 0.5$. This value (with rather large uncertainties) lies between the steep values predicted by CDM (-1.8 ; Mathis & White 2002) and the shallower values found observationally for galaxies in denser environments (-1.2 ; Blanton et al. 2003b, 2003c; Norberg et al. 2002b).

To accurately measure the LF of void galaxies, we examine a sample of 10^3 void galaxies selected from the SDSS. In our earlier work (Rojas et al. 2004), we found that these void galaxies are fainter, bluer, and have surface brightness profiles more similar to those of late-type galaxies. In Rojas et al. (2005), we found that void galaxies have higher specific star formation rates than objects in denser regions. In Goldberg et al. (2005) we used this sample to estimate the form of the mass function in voids, and found that the observed mass function is consistent in both shape and normalization with the mass function derived from extended Press-Schechter theory (Press & Schechter 1974; Bond et al. 1991; Mo & White 1996) in an underdense environment with $\delta\rho/\rho < -0.5$.

This paper is organized as follows. In § 2 we describe the selection of void galaxies from the SDSS. In § 3 we estimate the LF. We present the LF results in § 4. In § 5 we consider the LF of different subsamples of the data, selected by density, color, morphology, and star formation rate. In § 6 we discuss the results and compare them to other studies. We present conclusions in § 7.

2. THE VOID GALAXY SAMPLE

We identify a sample of 10^3 void galaxies from early data available from the SDSS. The SDSS is a wide-field photometric and spectroscopic survey that will cover approximately 10^4 deg^2 . CCD imaging of 10^8 galaxies in five colors and follow-up spectroscopy of 10^6 galaxies with $r < 17.77$ will be obtained. York et al. (2000) provide an overview of the SDSS, Stoughton et al. (2002) describe the early data release (EDR) and details of the photometric and spectroscopic measurements, and Abazajian

et al. (2003, 2004) describe the first (DR1) and second (DR2) data releases. Technical articles providing details of the SDSS include descriptions of the photometric camera (Gunn et al. 1998), photometric analysis (Lupton et al. 2002), the photometric system (Fukugita et al. 1996; Smith et al. 2002), the photometric monitor (Hogg et al. 2001), astrometric calibration (Pier et al. 2003), selection of the galaxy spectroscopic samples (Strauss et al. 2002; Eisenstein et al. 2001), and spectroscopic tiling (Blanton et al. 2003a). A thorough analysis of possible systematic uncertainties in the galaxy samples is described in Scranton et al. (2002). All the galaxies are K -corrected according to Blanton et al. (2003b), and we assume a $\Omega_m = 0.3$, $\Omega_\Lambda = 0.7$ cosmology and Hubble constant $h = H_0(100 \text{ km s}^{-1} \text{ Mpc}^{-1})^{-1}$ throughout.

Void galaxies are drawn from a sample referred to as “Sample10” (Blanton et al. 2003c). This sample covers nearly 2000 deg^2 and contains 155,126 galaxies. This sample is approximately 1.5 times that of the DR1 (Abazajian et al. 2003) and is contained in DR2 (Abazajian et al. 2004). We use a nearest-neighbor analysis, described in more detail below, to find galaxies that reside in regions of density contrast $\delta\rho/\rho < -0.6$ as measured on a scale of $7 h^{-1} \text{ Mpc}$, which we label void galaxies. Galaxies with larger values of $\delta\rho/\rho$ are referred to as wall galaxies. This choice of density contrast and nomenclature is consistent with our studies of voids in more three-dimensional samples, in which we are able to identify individual void structures using an objective *voidfinder* algorithm (Hoyle & Vogeley 2002, 2004) and to measure void sizes, average densities, and density profiles. This definition finds voids in the 2dFGRS, PSCz survey, and Updated Zwicky Catalog (UZC) with typical radii of $12.5 h^{-1} \text{ Mpc}$. These voids fill 40% of the universe and have mean density $\delta\rho/\rho < -0.9$. The average density around the few galaxies in voids (which typically lie closer to the edges) is typically $\delta\rho/\rho < -0.6$ when measured on a scale of $7 h^{-1} \text{ Mpc}$. Tests of these void-finding methods with CDM simulations and semi-analytic models (Benson et al. 2003a) indicate that we accurately identify the locations of true voids in the distributions of both galaxies and mass. In future, when deep, fully-three-dimensional samples from the SDSS are available, we will apply techniques such as *voidfinder* or tessellation techniques such as the Delaunay tessellation (F. Hoyle et al. 2005, in preparation) to objectively identify voids in this survey.

Details of void galaxy selection are described in Rojas et al. (2004). Here we provide a brief overview. First, a volume-limited sample of relatively bright galaxies is constructed to define the density field that traces the distribution of voids. This volume-limited sample extends to maximum redshift $z_{\text{max}} = 0.089$. We identify void galaxies from the flux-limited sample, also truncated at $z = 0.089$. We discard galaxies that lie close to the edge of the survey, because it is impossible to tell if a galaxy is a void galaxy if its neighbors could not yet have been observed. For each of the remaining galaxies in the flux-limited sample, we measure the distance to the third-nearest neighbor in the volume-limited catalog. A galaxy with fewer than three neighbors within a sphere of radius $7 h^{-1} \text{ Mpc}$ is flagged as a void galaxy. Galaxies with more than three neighbors are labeled wall galaxies. The void galaxies have local density contrast $\delta\rho/\rho \leq -0.6$. As expected, the density around void galaxies (ρ_{vg}) is higher than the mean density of a void ($\bar{\rho}_{\text{void}}$), because galaxies are clustered and the few void galaxies tend to lie close to the edges of the voids. This procedure yields a sample of 1010 void galaxies and 12,732 wall galaxies. These void and wall galaxies span a redshift range $0.034 \lesssim z < 0.089$. More importantly for the LF, the void galaxies span a range of magnitudes of $-22 < M_r < -17.77$. We show a histogram

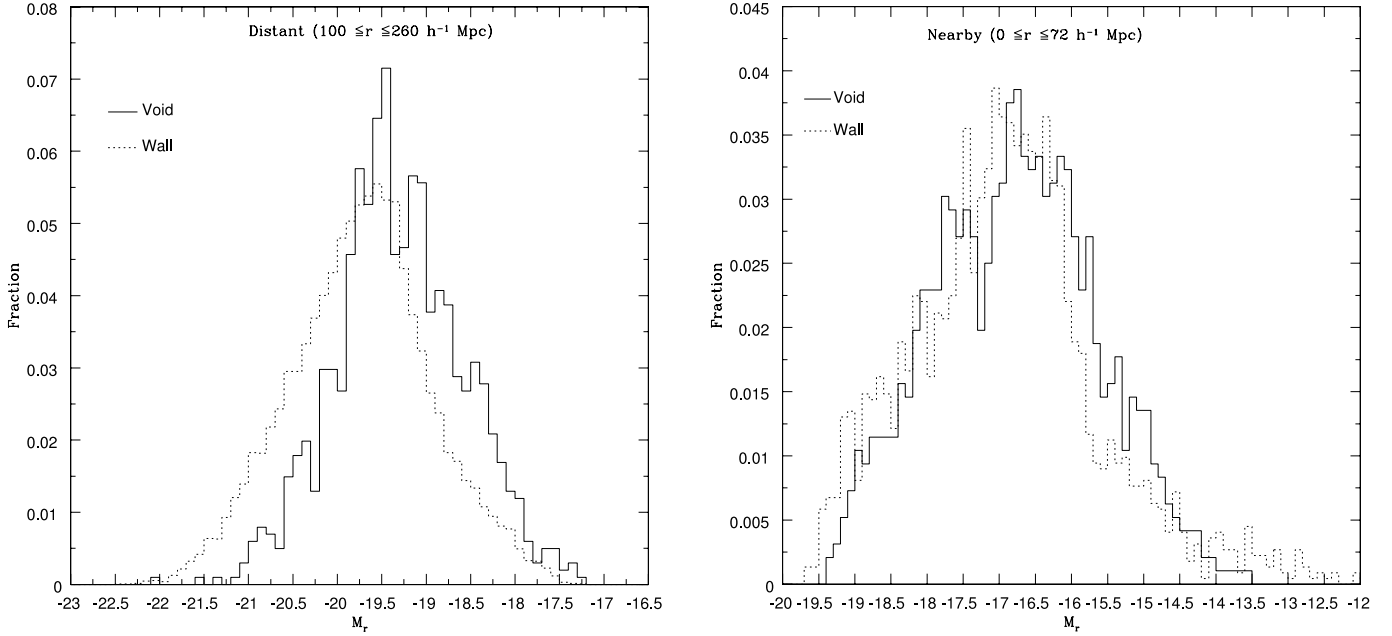


FIG. 1.—Distribution of absolute magnitudes in the distant (*left*) and nearby (*right*) wall (*dotted line*) and void (*solid line*) galaxy samples. The range of magnitudes probed by the distant void galaxies is $-22.0 \lesssim M_r \lesssim -17.77$. The nearby void galaxies cover the magnitude range $-19.7 \lesssim M_r \lesssim -13.0$. There are 1010 void and 12,732 wall galaxies in the distant sample and 194 void and 2256 wall galaxies in the nearby sample.

of these galaxies in the left panel of Figure 1. This sample is referred to as the “distant” sample.

We construct a sample of fainter and more nearby void galaxies (the “nearby” sample) by using the wider angle UZC (Falco et al. 1999) and the Southern Sky Redshift Survey (SSRS2; da Costa et al. 1998) to trace the distribution of local voids at distances where the slices of available SDSS scans, which extend over roughly 2.5° in declination, are too narrow to accurately map the large-scale structure (see Fig. 1 in Rojas et al. 2004). We construct volume-limited samples of the UZC and SSRS2 to match the density of objects used as tracers for the “distant” sample of SDSS galaxies. These nearby samples extend to maximum redshift $z_{\max} = 0.025$. We apply the same nearest-neighbor analysis and identify an additional 194 void galaxies and 2256 wall galaxies from a flux-limited sample of SDSS galaxies. The magnitudes of these galaxies lie in the range $-19.7 < M_r < -13$, shown in the right panel of Figure 1. For quantitative studies, we only use this sample down to $M_r = -14.5$, as there are only five galaxies fainter than this.

Below we estimate the LF for subsamples of void galaxies, selected by local density, color, surface brightness profile, and star formation rate, using SDSS measurements of these quantities. SDSS magnitudes are Petrosian magnitudes (Petrosian 1976), which measure the total amount of flux within a circular aperture whose radius depends on the shape of the galaxy light profile, i.e., the angular aperture varies such that galaxy fluxes are measured within the same physical aperture at all redshift for objects of the same type. More details are given in Stoughton et al. (2002). Colors of galaxies are also computed using Petrosian magnitudes. Below we split the sample by color using the highest signal-to-noise ratio color available, $g-r$. To estimate the form of the surface brightness profile we use Sérsic indices (Sérsic 1968) measured by Blanton et al. (2003c). The Sérsic index, n , is found by fitting the functional form $I(r) = I_0 \exp(-r^{1/n})$ to the surface brightness profile of each galaxy. A value of $n = 1$ corresponds to a purely exponential profile, while $n = 4$ is a de Vaucouleurs profile. The final property on which we split the sample is the star

formation rate, as measured by the strength of the $H\alpha$ emission line. Rojas et al. (2005) find that, on average, the equivalent widths of $H\alpha$, $H\beta$, $O\text{ II}$, and $N\text{ II}$ are larger for void galaxies than for wall galaxies in all of these lines. Again, we choose $H\alpha$ for selecting subsamples because it typically has the largest signal-to-noise ratio.

3. ESTIMATING THE LUMINOSITY FUNCTION

3.1. Method

We present estimates of the LF using the maximum likelihood approach of Efstathiou et al. (1988; SWML). We obtain similar results using the V_{\max} method (Schmidt 1968), except at the faint end where the V_{\max} method is known to be a poor estimator owing to sample variance.

The results we present are in the form of the magnitude function, $\Phi(M)$, which is related to the LF through the relation $\Phi(L)dL = \Phi(M)dM$. For each measurement of the LF, we find the parameters of the Schechter (1976) function,

$$\Phi(L) = (\Phi^*/L^*)(L/L^*)^\alpha \exp(-L/L^*), \quad (1)$$

that best fit the data. In magnitudes, this function takes the form

$$\Phi(M) = (0.4 \ln 10) \Phi^* 10^{0.4(\alpha+1)(M^*-M)} \exp(-10^{0.4(M^*-M)}). \quad (2)$$

We estimate the best-fit normalization Φ^* , the characteristic magnitude M_r^* , and faint-end slope α by minimizing χ^2 of the fit to our data (see § 3.2 for estimates of the uncertainties). For each measurement of the LF, we fit the Schechter function twice: the first time, all three parameters are allowed to vary, to obtain an estimate of M_r^* . The second time, we fit the three parameters again but restrict the range of the fit to $M_r^* - 1 < M_r < M_r^* + 5$, to ensure we are fitting the Schechter function to the same part of the LF for each subsample. We find that the estimates of α are the most sensitive to the range of magnitudes over which the fits are performed, although the values of α found by fitting over the

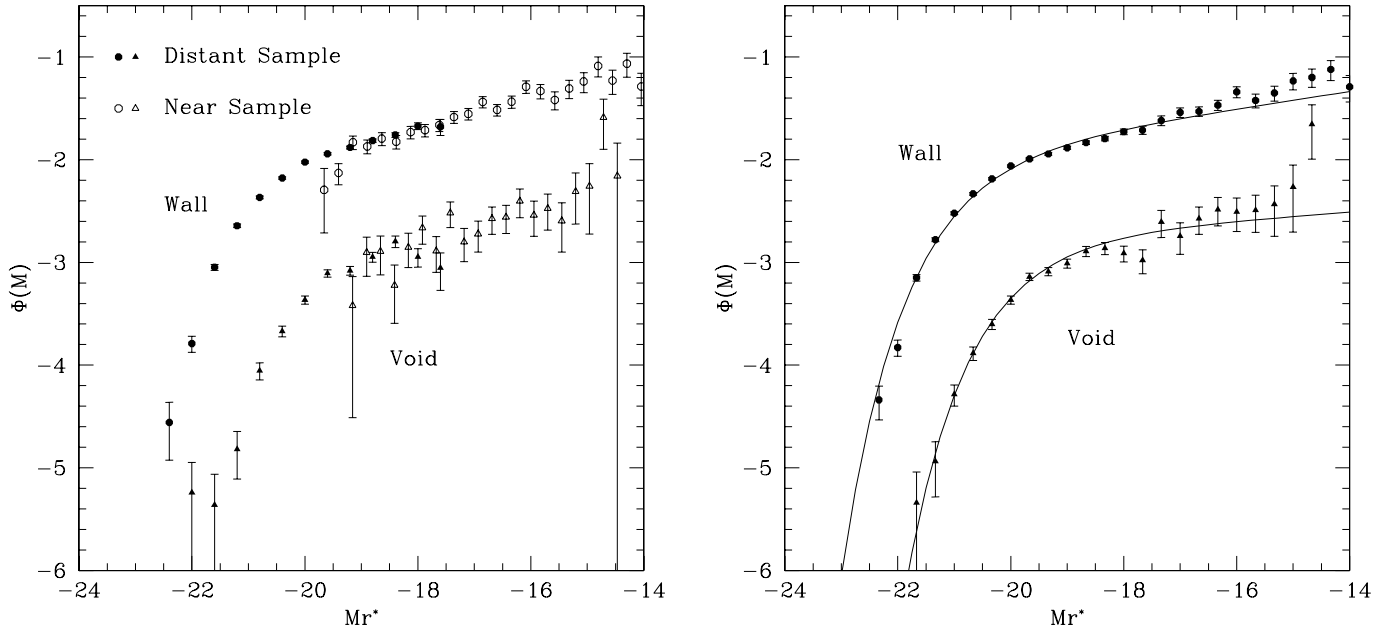


FIG. 2.—LFs of void and wall galaxy samples. *Left*: LFs of the distant (*filled points*) and nearby (*open points*), void (*triangles*) and wall (*circles*) galaxy samples. *Right*: Combined LFs of the full void (*triangles*) and wall (*circles*) galaxy samples. The solid line shows the best-fit Schechter function to each sample. The fitted parameters are listed in Table 1.

restricted range and the full range of magnitudes agree within 1σ .

We separately measure the LF of the distant and nearby, void and wall galaxy subsamples. Then we combine the distant and nearby LFs, using an error-weighted average of the measurements in the region of overlap. We normalize the LFs of the wall and void galaxy samples to match the number per square degree of galaxies that would be predicted from the full SDSS sample. Approximately 11/12 of the galaxies are wall galaxies and 1/12 are void galaxies (Rojas et al. 2004).

3.2. Errors

We use two methods to estimate the uncertainties in our LF measurements. The first method is that of Efstathiou et al. (1988), which uses the property that the maximum likelihood estimates of Φ are asymptotically normally distributed. The second method is the jackknife method (Lupton 1993). We implement the jackknife method by constructing 18 subsamples of the galaxies. Each subsample excludes a different 1/18 of the area of the survey. We then measure the LF of each subsample and estimate the error of the full sample using the formula

$$\text{Var}(x) = \frac{N-1}{N} \sum_{i=1}^N [x - (\bar{x})]^2, \quad (3)$$

where N is the number of subsamples. These two methods yield similar error estimates (see Fig. 3 below).

4. LUMINOSITY FUNCTIONS OF VOID AND WALL GALAXIES

In Figure 2 we present the LFs of the void and wall galaxy samples. Note that, by combining the nearby and distant samples, we are able to measure the LF of void galaxies over a wide range of M_r values, $-21.5 < M_r < -14.5$. The inclusion of the nearby sample allows us to probe 2 mag fainter than other studies of void galaxies. The amplitudes of the nearby and distant LFs agree over the range in which they probe the same range of

absolute magnitude. In the left panel, we plot separate symbols for the LFs of the nearby (*open symbols*) and distant (*filled symbols*) samples of void (*triangles*) and wall (*circles*) galaxies. In the right panel of Figure 2, we plot the void (*triangles*) and wall (*circles*) LFs after combining the nearby and distant sample LFs for each. The plotted uncertainties are computed using the method of Efstathiou et al. (1988). Solid lines show the best-fit Schechter function curves, as discussed below.

In Figure 3 we compare the errors found using the Efstathiou et al. (1988) and jackknife methods. We plot the fractional error estimated by both methods for each galaxy sample. These two error estimates are very similar, particularly over the range of absolute magnitude in which the LF is accurately measured. The amplitude of jackknife errors shows larger variation from point to point, whereas the Efstathiou et al. errors follow a smoother trend. Hereafter, we use only the Efstathiou et al. errors for fits to the data.

We fit a Schechter function to the various LFs, as described in § 3. In the case of the void galaxies, a Schechter function is a good fit to the LF, with χ^2 per degree of freedom close to 1. The wall galaxy LF shows a somewhat poorer fit for the distant and combined samples; χ^2 per degree of freedom is as large as 2.3. The relatively poorer fit for the wall galaxy LF may simply reflect the smaller errors admitted by the larger number of wall galaxies, rather than an intrinsic property of the population. It should be noted that both the void and wall galaxy LFs rise above the Schechter function fit at the faint end. A different form for the LF may fit better. For example, Trentham & Tully (2002) suggest that a six-parameter model would better fit their cluster LFs.

The combined void galaxy sample has best-fit parameters of $\Phi^* = (0.19 \pm 0.04) \times 10^{-2} h^3 \text{Mpc}^{-3}$, $M_r^* - 5 \log h = -19.74 \pm 0.11$, and $\alpha = -1.18 \pm 0.13$. For comparison, the combined wall galaxy sample has best-fit parameters of $\Phi^* = (1.42 \pm 0.3) \times 10^{-2} h^3 \text{Mpc}^{-3}$, $M_r^* - 5 \log h = -20.62 \pm 0.08$, and $\alpha = -1.19 \pm 0.07$. Table 1 lists the parameters and goodness of fit for each sample. These values are used to plot the Schechter function curves shown in the right panel of Figure 2.

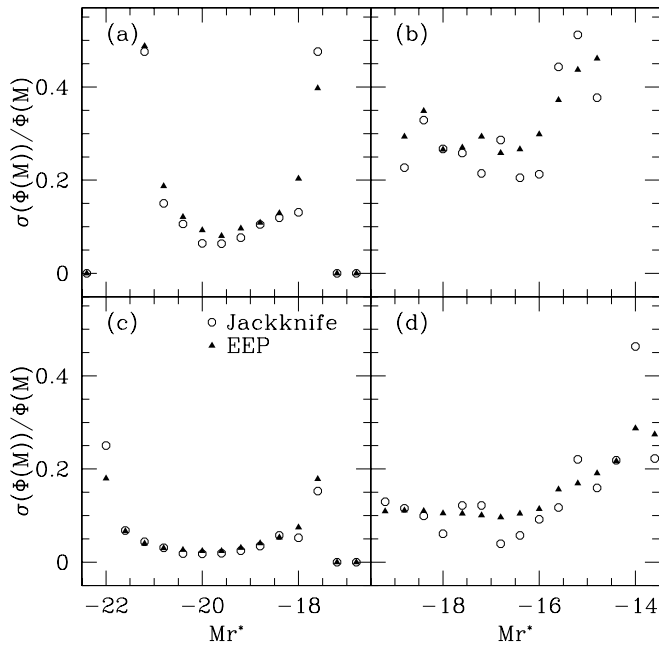


FIG. 3.—Comparison of error estimation techniques. Plotted are the fractional errors calculated using the method of Efstathiou et al. (1988; *triangles*) and the jackknife method (*circles*), as described in § 3.2, for the (a) void distant sample, (b) void nearby sample, (c) wall distant sample, and (d) wall nearby sample. The errors are smaller for the distant samples because of the larger number of galaxies. Both methods give similar sized errors, although the jackknife errors exhibit more scatter.

In Figure 4, we plot two-dimensional uncertainty contours of M_r^* and α , keeping Φ^* fixed at the best-fit value for each combined sample. We note that these contours show only mild degeneracy between α and M_r^* , because our nearby sample of void galaxies allows the LF to be measured down to quite faint magnitudes; thus, α is relatively better determined than in previous studies. The faint-end slopes of void and wall galaxies agree within these uncertainties. However, M_r^* of the void galaxy sample is fainter than for the wall galaxy sample by many standard deviations. This result agrees with that obtained by Rojas et al. (2004), who use a Kolmogorov-Smirnov test to compare the distributions of absolute magnitudes.

The Schechter function parameters of the combined wall sample agree with those of the SDSS Early Data Release (EDR) sample examined by Blanton et al. (2001), who estimated $\Phi^* = (1.46 \pm 0.12) \times 10^{-2} h^3 \text{ Mpc}^{-3}$, $M_r^* - 5 \log h = -20.83 \pm 0.03$, and $\alpha = -1.20 \pm 0.03$, corrected to rest-frame magnitudes at $z = 0$. Blanton et al. (2003b) estimated the LF with magnitudes

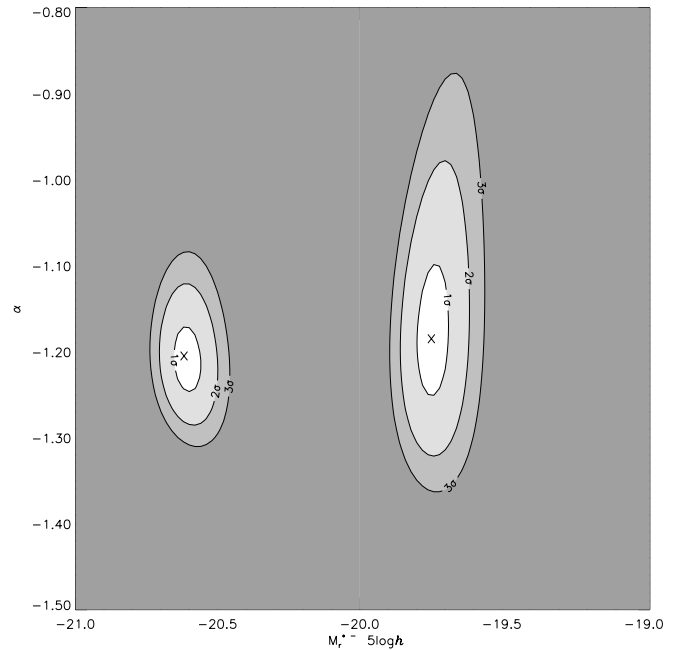


FIG. 4.—Uncertainty ranges (1, 2, and 3 σ) of Schechter function parameter fits to the void and wall galaxy LFs. The contours with the smaller error range on the left are for the wall galaxy sample. The contours on the right are for the void galaxies. The two crosses indicate the best-fit values of $M_r^* - 5 \log h$ and α . For the void galaxies, these are $M_r^* = -19.74$ and $\alpha = -1.18$ when Φ^* is fixed at $0.0019 h^3 \text{ Mpc}^{-3}$. For the wall galaxies, the central values are $M_r^* = -20.62$ and $\alpha = -1.19$ with Φ^* fixed at $0.014 h^3 \text{ Mpc}^{-3}$.

corrected to rest frame at $z = 0.1$ from galaxies in Sample10 and found with best-fit values of $\Phi^* = (1.49 \pm 0.04) \times 10^{-2} h^3 \text{ Mpc}^{-3}$, $M_r^* - 5 \log h = -20.44 \pm 0.01$, and $\alpha = -1.05 \pm 0.01$. The difference between the values of α found in the latter two papers is explained in Figure 15 of Blanton et al. (2003b). They attribute the difference to a modest luminosity evolution correction. Because all the galaxies in our sample lie at redshifts $z < 0.1$ and the galaxies in the nearby sample are at redshifts $z < 0.025$, we do not apply the evolution correction.

We carefully examine the possible influence on our Schechter function fits of errors in our procedure for combining the LFs of the nearby and distant samples. First, we fit the distant samples and nearby samples independently. These parameter values are listed in Table 1. In the distant sample cases, the values of α are not well determined. In the nearby sample cases, Φ^* and M_r^* are not well determined. These large uncertainties are clearly the result of the narrow range of luminosity probed by the nearby and distant samples individually. Note, however, that the values

TABLE 1
SCHECHTER FUNCTION FITS TO THE VOID AND WALL LFs OF THE COMBINED, DISTANT, AND NEAR SAMPLES

Sample	Φ^* ($\times 10^{-2} h^3 \text{ Mpc}^{-3}$)	$M_r^* - 5 \log h$	α	χ^2/ν
Void Combined	0.19 ± 0.04	-19.74 ± 0.11	-1.18 ± 0.13	0.9
Void Distant	0.20 ± 0.08	-19.68 ± 0.18	-0.97 ± 0.23	1.1
Void Nearby	0.31 ± 0.21	-20.10 ± 1.90	-1.25 ± 0.15	0.5
Wall Combined	1.42 ± 0.3	-20.62 ± 0.08	-1.19 ± 0.07	1.9
Wall Distant	1.79 ± 0.6	-20.40 ± 0.14	-1.03 ± 0.16	2.3
Wall Nearby	4.20 ± 1.2	-18.55 ± 1.29	-1.15 ± 0.12	0.7

NOTE.—Fits to the void and wall LFs of the combined (distant and near LFs combined into one LF), distant, and near samples, found by minimizing χ^2 . The distant samples alone can constrain Φ^* and M_r^* well but cannot place strict limits on α , whereas the nearby samples constrain α better.

of α from the nearby samples agree well with those from the combined samples and that the values of Φ^* and M_r^* from the distant samples agree well with those from the combined samples. We also note that there is a dip in the void galaxy LF around -17.5 . This is where the distant and nearby samples are matched together. Therefore, as a second test of the reliability of the Schechter function parameters, we remove the points in the range $-18 < M_r < -16.7$ and refit the combined void LF. We find that the Schechter function parameters agree within 1σ with those found from fitting the whole LF. Thus, combining the nearby and distant LFs does not significantly change the Schechter function parameter estimation. We note that the completed SDSS will allow measurement of the LF of void galaxies over the full range of absolute magnitude, using a contiguous range of redshift and without the use of other samples to map the nearby void distribution.

5. LUMINOSITY FUNCTION DEPENDENCE ON DENSITY AND INTRINSIC PROPERTIES

5.1. Density Dependence

We examine variation of the LF with environment in more detail by estimating LFs for density-selected subsamples of the void and wall galaxy samples.

We again use the distance to the third-nearest neighbor as a measure of the local density, and split both the void and wall galaxy samples at the median value to form high- and low-density subsamples of each void and wall galaxy sample. The void galaxies all have a distance to the third-nearest neighbor, $d_3 > 7 h^{-1}$ Mpc, which corresponds to density contrast of $\delta\rho/\rho < -0.6$. We split the void galaxy samples at $d_3 = 8.38 h^{-1}$ Mpc, which results in a density contrast range of $\delta\rho/\rho < -0.75$ for the lower density subsample and $-0.75 < \delta\rho/\rho < -0.6$ for the higher density subsample. We split the wall galaxy sample at the median distance to the third-nearest neighbor, $d_3 = 3.96 h^{-1}$ Mpc. Thus, the lower density wall sample spans the density contrast $-0.6 < \delta\rho/\rho < 1$, and the higher density wall galaxy includes density contrast $1 < \delta\rho/\rho$. To yield comparable uncertainties for the LFs of these void and wall galaxy subsamples, we sparse-sample the wall galaxy samples to contain just 500 wall galaxies, which matches the number of void galaxies in the density-selected subsamples.

We plot the LFs of the density-selected subsamples in Figure 5. As we examine subsamples of increasing density, from the low-density void sample up to the high-density wall sample, we see a clear trend of brighter values of $M_r^* - 5 \log h$ (~ -19.70 , -19.80 , -20.20 , -20.40 ± 0.15 , respectively). However, the faint-end LF slopes of both the low- and high-density void sample and low-density wall sample are similar ($\alpha \sim -1.15 \pm 0.20$); the LF of the wall galaxies in the highest density sample has a somewhat different shape, with a relatively shallow faint-end slope of $\alpha = -0.92 \pm 0.20$. The pronounced shape difference for this densest sample may be caused by the strong type dependence of galaxies near clusters and groups (e.g., Dressler 1980; Postman & Geller 1984).

5.2. Dependence on Color, Profile, and Star Formation Rate

The dependence of the LF on density prompts us to examine whether this variation is caused by variation of the type of galaxies with environment. We would like to study the void galaxy LF as a function of photometric and spectroscopic parameters such as color, surface brightness profile (SBP), and line widths. As we show in Rojas et al. (2004, 2005), the void galaxies span a relatively narrow range of these properties: they

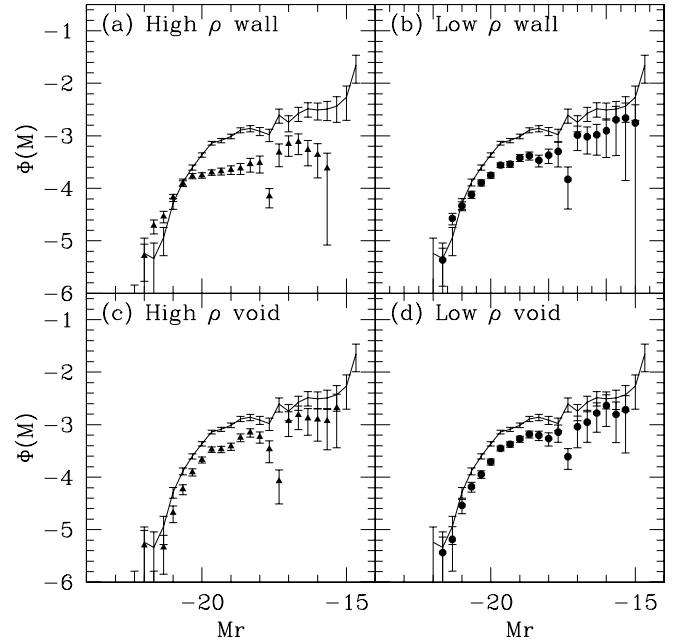


FIG. 5.—LFs of galaxies as a function of density. Shown are (a) the LF of the highest density wall galaxies ($1 \lesssim \delta\rho/\rho$), (b) the lowest density wall galaxies ($-0.5 \lesssim \delta\rho/\rho \lesssim 1$), (c) the highest density void galaxies ($-0.75 \lesssim \delta\rho/\rho \lesssim -0.6$), and (d) the lowest density void galaxies ($\delta\rho/\rho \lesssim -0.75$). The solid line is the void galaxy LF.

are blue (mean $g - r = 0.615 \pm 0.007$ void vs. 0.720 ± 0.002 wall), have small ($n < 2$) Sérsic indices (mean 1.718 ± 0.024 void vs. 2.051 ± 0.002 wall), and have strong equivalent widths (mean 19.14 ± 0.68 void vs. 11.77 ± 0.16 wall). Splitting the void galaxy sample into several bins of an intrinsic property would also yield small subsamples. However, instead we split the larger wall galaxy sample, and examine whether the void galaxy sample is similar to any of the wall galaxy subsamples. We split the wall galaxy samples to create pairs of subsamples that have intrinsic properties that are similar or dissimilar to the void galaxies: we split by color at $g - r = 0.75$, Sérsic index at $n = 2$, and $H\alpha$ equivalent width of 5 \AA , which are close to the median values, and measure the LF of the six subsamples of wall galaxies.

In Figure 6 we plot the LF of the wall galaxy subsamples with properties similar to those of void galaxies (*open circles*), and the LF of the wall galaxies with properties dissimilar to those of void galaxies (*filled circles*), together with the LF of the full void and wall galaxy samples, as shown in Figure 2. To aid comparison of the void and wall galaxy LFs, we also plot the void galaxy LF multiplied by a factor of 11, which approximately matches the amplitude of the wall galaxy LF, as there are ~ 11 times as many wall galaxies as void galaxies in the full sample. The left panel shows the LFs of blue versus red wall galaxies, the center panel plots the LFs of wall galaxies with early-type versus late-type surface brightness profiles, and the right panel shows the LFs of wall galaxies with strong versus weak $H\alpha$ emission.

Figure 7 clearly explains why the three panels of Figure 6 appear so similar: the cuts we make on color, Sérsic index, and $H\alpha$ equivalent width to select voidlike wall galaxies yield nearly, but not quite the same, wall galaxies in each case. Thus, 3500 of the ~ 5000 galaxies in each sample are the same. In detail, we do see some differences between the LFs, as discussed below. As above, we fit a Schechter function to each LF. Table 2 summarizes these parameter fits.

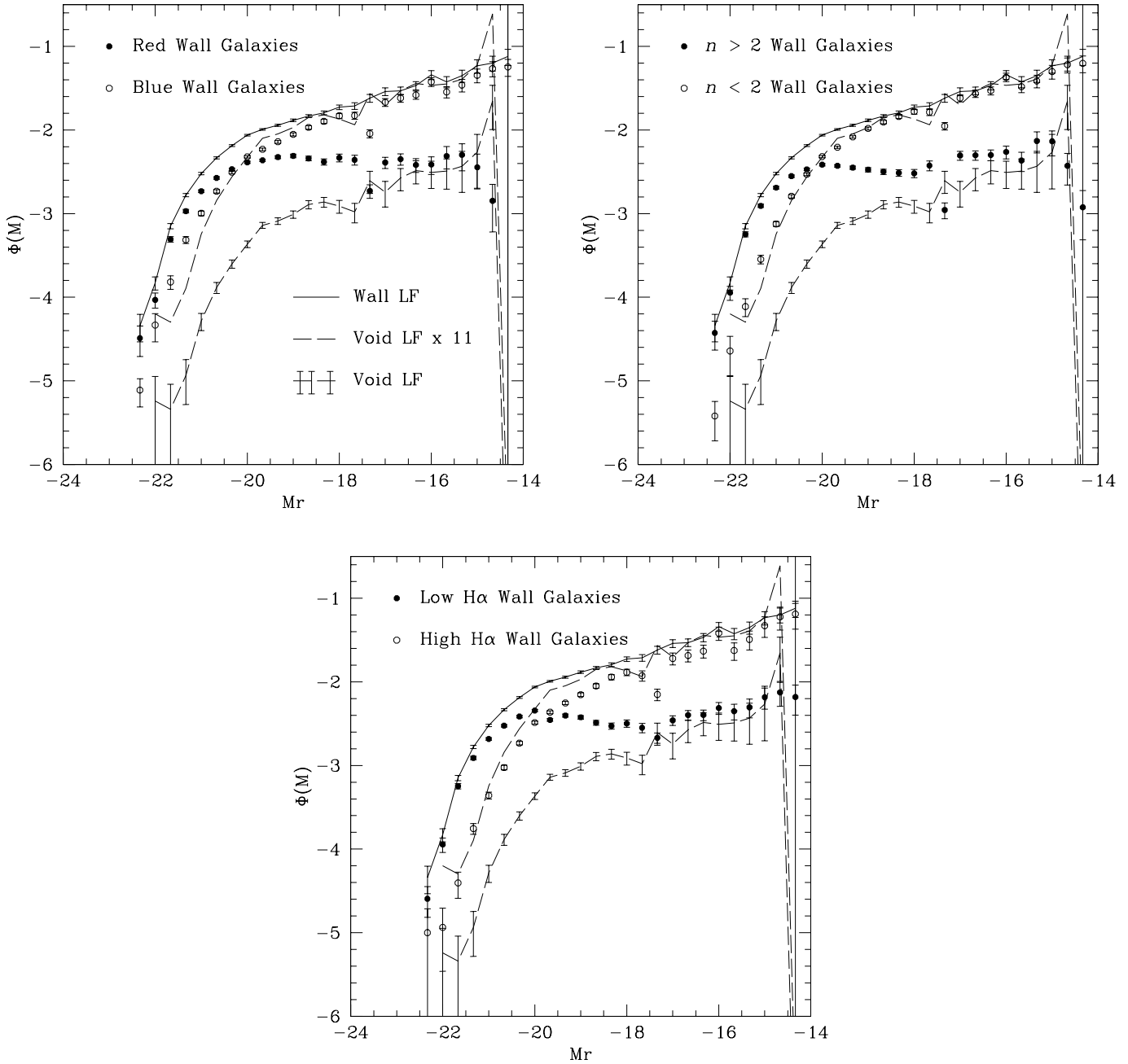


FIG. 6.—LFs of wall galaxies split by color (*top left*), Sérsic index (*top right*), and strength of H α equivalent width (*bottom*). Open circles show the LFs of wall galaxies with properties that are generally associated with late-type galaxies. Filled circles show the LFs of wall galaxies with properties that are generally associated with early-type galaxies. Solid lines show the LF of the wall galaxies. Dashed lines with error bars show the LF of the void galaxies. Higher amplitude dashed lines without error bars show the LF of the void galaxies multiplied by 11, to approximately match the amplitude of the wall galaxy LF.

The blue, low Sérsic index, and high H α wall galaxy LFs all have faint-end slopes of $\alpha \approx -1.3 \pm 0.1$. The low Sérsic index and high H α LFs have values of $M_r^* \approx -20.0 \pm 0.15$, while the blue subsample is slightly brighter, with $M_r^* = -20.34 \pm 0.15$. The Schechter function is an excellent fit to all three LFs, with $\chi^2/\nu \approx 1$.

The void galaxy LF (for comparison we use our best estimate, that of the “combined” LF) has faint-end slope $\alpha \approx -1.2$, within 1σ of the slope measured for these “void galaxy-like” wall galaxies. The void galaxy LF is strongly shifted toward fainter magnitudes by roughly $2\text{--}5 \sigma$ compared to the wall galaxy LFs. The closest match to the void galaxy LF is that of the high-H α wall galaxy subsample. Thus, while the shape of the “void galaxy-like” wall galaxies is similar to that of void

galaxies, the shift of luminosity found by Rojas et al. (2004) persists.

The LFs of red, high Sérsic index, and low-H α “unvoid-like” wall galaxy subsamples all have relatively bright values of $M_r^* \approx -20.35 \pm 0.14$. The faint ends of the high Sérsic index and low H α LFs are very flat, with $\alpha \approx -0.5 \pm 0.3$, while the red subsample has only very slightly steeper slope, $\alpha \approx -0.7 \pm 0.2$. The Schechter function is a poor fit to the LFs of these unvoid-like samples; χ^2 per degree of freedom ranges from 5 to 8 for these fits. Keeping in mind the poor fit, we note that these LFs have M_r^* that are many standard deviations brighter, and faint-end slopes α that are significantly flatter than the LFs of either the void galaxy-like wall galaxies or the void galaxies themselves. It is not surprising to find that the LFs of

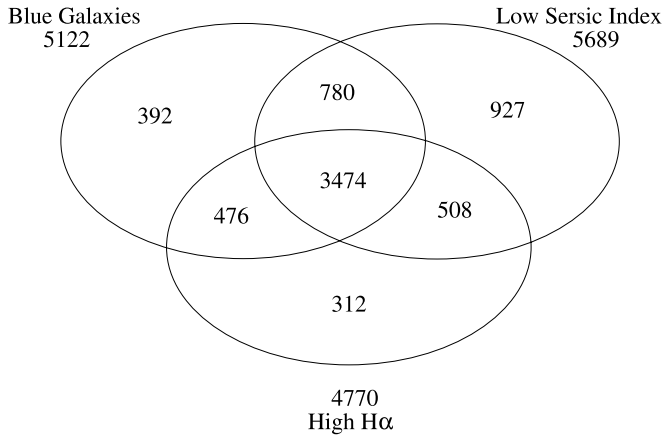


FIG. 7.—Venn diagram illustrating the number of wall galaxies in subsamples selected to have colors, Sérsic indices, or $H\alpha$ equivalent widths that are generally associated with late-type galaxies. Roughly 60% of the galaxies are common to all three subsamples; thus, the LFs of these subsamples should be similar.

wall galaxies with properties dissimilar to the void galaxies are strikingly different from the void galaxy LF in both shape and scale, because those subsamples are at the other extreme of both environment and intrinsic properties.

Thus, we find that the LFs of wall galaxies with more void galaxy-like properties (blue $g-r$ color, late-type profile, or large $H\alpha$ equivalent width) appear most similar to the LF of the void galaxies, but we do not find such a wall galaxy subsample that matches both the faint-end slope α and characteristic magnitude M_r^* of the void galaxies. Neither do we find a density-selected subsample of wall galaxies that matched the void galaxy LF. This set of comparisons supports the conclusions of Rojas et al. (2004, 2005) that, on average, the void galaxy population is bluer, fainter, has later-type surface brightness profiles, and exhibits stronger specific star formation rates than galaxies in denser regions. This trend is caused both by the dominance of blue over red galaxies at low density and by the tendency for late-type galaxies in voids to be bluer and fainter than galaxies of similar morphological type in denser regions. In other words, although the distribution of intrinsic properties of void galaxies is most similar to that of late-type galaxies in environments modestly denser than the voids, and is partially explained by a strong “demographic” shift toward later types, the distribution of void galaxy properties cannot be simply explained by extrapolation of the morphology-density relation into voids, because there is also a marked trend with decreasing density toward lower luminosity and bluer color among galaxies of the same morphology.

6. COMPARISON WITH PREVIOUS OBSERVATIONS AND SIMULATIONS

In this section, we compare our estimate of the void galaxy LF to the LFs of other galaxy samples probing a range of types and environments. We then discuss our results vis-à-vis theoretical models for galaxy formation.

6.1. Observed Variations with Environment and Type

The void galaxy LF was first measured by Grogin & Geller (1999) for a sample of 149 void galaxies with local density contrast below the mean ($\delta\rho/\rho < 0$). For this sample, they found a best-fit Schechter function with shallow faint-end slope of $\alpha = -0.5 \pm 0.3$ in the B band and -0.9 ± 0.3 in the Century R band. Estimating the LF for 46 galaxies with density contrast $\delta\rho/\rho < -0.5$, they found a LF with very steep faint-end slope of $\alpha = -1.4 \pm 0.5$. The LF of our sample of 10^3 void galaxies, in slightly lower density environments ($\delta\rho/\rho < -0.6$), has a faint-end slope of $\alpha \approx -1.2$, consistent within the large uncertainties of the earlier study.

The LF of galaxies found in more typical environments has been accurately measured from both the SDSS (Blanton et al. 2003b, 2003c) and the 2dFGRS (Norberg et al. 2002b). The values of α obtained by these two surveys are similar to the values we find for the void galaxies, roughly $\alpha = -1.20 \pm 0.03$. The values of M_r^* fitted to the LF of the full surveys are approximately 1 mag brighter than our void galaxy LF. Blanton et al. (2005) have also considered the LF of faint galaxies in average galaxy environments and find similar faint-end slopes but a shift in the value of M^* with environment.

The LF has also been measured in higher density samples. Trentham & Tully (2002) studied the LF in nearby groups and clusters of galaxies such as the Virgo Cluster, Coma I Group, Leo Group, and two NGC groups. They found that a Schechter function is not a good fit to the measured LF, as there appears to be a change in the shape of the LF around $M_R = -18$, which the Schechter function does not account for. This feature is also seen in our LFs, but because the distant and nearby samples are matched around this magnitude, it is difficult for us to assess its reality (although we do test, in § 4, that our LF fits do not change when this range of absolute magnitude is excluded). It will be interesting to see if this shape change persists when the SDSS is finished and the LF is measured over a wide range of magnitudes, without the need to match the LFs of distant and nearby samples (see § 3 above). Trentham & Tully conclude that, although the Schechter function is a poor fit, a faint-end slope of $\alpha \sim -1.2$ is consistent with all of the groups considered in their study.

Bromley et al. (1998) measure the LF of the Las Campanas Redshift Survey (LCRS) as a function of density, and Hütsi

TABLE 2
SCHECHTER FUNCTION FITS TO THE WALL GALAXY LFs SPLIT BY COLOR, SÉRSIC INDEX, AND STRENGTH OF THE $H\alpha$ EMISSION

Sample	Φ^* ($\times 10^{-2} h^3 \text{ Mpc}^{-3}$)	$M_r^* - 5 \log h$	α	χ^2/ν
Blue ($g-r < 0.75$).....	0.90 ± 0.5	-20.34 ± 0.14	-1.32 ± 0.11	1.0
Sérsic index $n < 2$	1.30 ± 0.6	-20.02 ± 0.16	-1.28 ± 0.10	0.9
EW($H\alpha$) $> 5 \text{ \AA}$	0.90 ± 0.5	-19.98 ± 0.17	-1.32 ± 0.11	1.0
Red ($g-r > 0.75$).....	0.98 ± 0.5	-20.38 ± 0.12	-0.73 ± 0.21	4.8
Sérsic index $n > 2$	0.98 ± 0.5	-20.34 ± 0.14	-0.51 ± 0.32	8.0
EW($H\alpha$) $< 5 \text{ \AA}$	1.00 ± 0.6	-20.36 ± 0.14	-0.55 ± 0.35	7.8

NOTE.—The fits are made to the LFs shown in Figure 6 and described in § 5.

et al. (2003) similarly consider the LF of the LCRS and SDSS. They both conclude that there is little change in the values obtained for α from the LFs of late-type galaxies in differing environments. Hütsi et al. (2003) see a shift in M^* with density but did not probe the LF of the most underdense regions.

In addition to the environmental dependence of the LF, we can consider the morphological dependence of the LF. Nakamura et al. (2003) measured by eye the morphology of 1482 SDSS galaxies with magnitudes in the range $-23 < M_r^* < -18$. They present the LFs of their galaxies as a function of morphology and as a function of the inverse concentration index, which is defined as the ratio of two Petrosian radii, $C = r_{50}/r_{90}$. Nakamura et al. find that concentrated galaxies have a LF with faint-end slope of $\alpha = -1.12 \pm 0.18$, whereas less concentrated galaxies have a flatter faint-end slope of $\alpha = -0.68 \pm 0.23$. We do not have morphologies for all the galaxies in our sample, but the concentration index has been measured. Rojas et al. (2004) find that the void galaxies are more concentrated than the wall galaxies; thus, we expect consistency between the faint-end slope of the void galaxy LF and the concentrated galaxies LF of Nakamura et al. The value of M^* for the concentrated galaxies in Nakamura et al., $M^* = 20.35 \pm 0.19$, is brighter than the void galaxy value, most likely owing to the paucity of bright, early-type galaxies in voids. The LF of the concentrated galaxies is very similar in shape to the LF of the Sa, Sb sample in Nakamura et al.

Madgwick et al. (2002) measure the LF of the galaxies in the 2dFGRS as a function of star formation activity, as determined by the strength of emission lines. They find that the LF of the most passive galaxies has a shallow faint-end slope of -0.54 ± 0.02 , whereas the LF of the most active star-forming galaxies has a steep slope of -1.50 ± 0.03 . Rojas et al. (2005) find that void galaxies have fairly strong emission lines and higher star formation rates than wall galaxies; hence their blueness. However, these void galaxies do not have star formation rates quite as high as the most extreme sample of Madgwick et al., which may explain why the void galaxy LF has a somewhat shallower faint-end slope ($\alpha \approx -1.2$ vs. -1.5).

Shortly before publication, we received results from the 2dFGRS group on the LF of galaxies as a function of environment in that survey. Croton et al. (2005) define a void galaxy sample with $\delta < -0.75$, a mean sample with $-0.43 < \delta < 0.32$, and a high-density sample with $\delta > 6$. They find that the LF of the void galaxies has a faint-end slope similar to their mean sample but, in agreement with our results, that M^* is fainter for the void galaxies and brighter for the high-density sample. Thus, they also find that there is little change in α as a function of environment, but that M^* brightens as the local density increases. Our estimates of the LF at the faint end, extending to $M_r = -15$ versus $M_{b,r} = -17$ for the 2dFGRS, more accurately determine α , thus constraining variation at low density. Examining subsamples divided into late and early types using spectral line widths, they find that the void galaxy sample is dominated by late-type galaxies, whereas the high-density sample is dominated by early-type galaxies, consistent with our findings.

To summarize, it appears observationally that the LF of the void galaxies has a value of α that is consistent with other samples of galaxies that reside in somewhat higher density environments. The faint-end slope of the void galaxy LF is very similar to the LF of late-type galaxies, concentrated galaxies, and galaxies with moderate star formation rates. The value of M_r^* from the void galaxy LF is fainter than for the LFs of galaxies with similar concentration indices and star formation rates. This suggests that the difference in the LF is caused by a paucity of bright galaxies in the void regions, consistent

with a shift in the halo mass function (see, e.g., Goldberg et al. 2005).

6.2. Predictions from CDM Models

The mass function of dark matter halos in voids shifts to much lower masses (Sheth & Tormen 2002; Gottlöber et al. 2003; Goldberg et al. 2005); thus, CDM models predict a relatively larger number of low-mass halos in voids. However, the existence of dwarf galaxies in voids is sensitive to the details for baryon cooling, star formation, and feedback effects. Benson et al. (2003b) have investigated the effects of photoionization on the shape of the LF. They conclude that feedback, in the form of supernova-driven winds and photoionization, can significantly flatten the faint-end slope of the LF. Benson et al. also note the ‘‘hump’’ around $M = -17$ in the LF of smaller mass halos of ($M < 10^{13} h^{-1} M_\odot$) and attribute that feature to the relative contribution of central and satellite galaxies, i.e., at magnitudes fainter than $M = -17$, satellite galaxies are more numerous than central galaxies.

In particular, void galaxies have been studied using CDM simulations plus semianalytic models by Mathis & White (2002). They extracted mock galaxy catalogs from high-resolution Λ CDM plus semianalytic simulations. They measure the LF as a function of environment, splitting the catalogs by both mass and volume. They find that there are no very bright galaxies in voids and that the slopes of the LFs do not change greatly with environment. Their predicted values of the faint-end slopes are $\alpha \approx -1.4$ in the high-density environments and $\alpha \approx -1.6$ in the low-density environments. Both of these values are steeper than observed, although the trend of α is in the same sense as we find in Figure 5, i.e., LFs measured from lower density galaxies are steeper than LFs from galaxies in the highest density environments. Mathis & White point out that for a void galaxy LF to have a steeper slope, the void region would have to be populated by faint, dwarf galaxies. However, it does not appear that there is a large excess of dwarf galaxies in void regions (Binggelli 1989; Kuhn et al. 1997; Popescu et al. 1997), consistent with our observed void galaxy LF.

7. CONCLUSIONS

Using the sample of void galaxies obtained by Rojas et al. (2004), we measure the luminosity function (LF) from a sample of 10^3 void galaxies that cover a wide range of magnitude, $-21.5 < M_r < -14.5$. We summarize our conclusions, as follows.

1. The void galaxy LF is well fitted by a Schechter function with parameters $\Phi^* = 0.0019 \pm 0.0004 h^3 \text{ Mpc}^{-3}$, $M_r^* - 5 \log h = 19.74 \pm 0.11$, and $\alpha = -1.18 \pm 0.13$. This value of M_r^* is approximately 1 mag fainter than that of the wall galaxy sample. This luminosity difference is consistent with the result of Rojas et al. (2004), who find that void galaxies are fainter than wall galaxies. We split the void and wall galaxy samples in half by density and reestimate the Schechter function parameters. We find a steady increase with local density of the brightness of M_r^* .

2. The faint-end slope α of the void galaxy LF is consistent with the wall galaxy LF value and with the values measured for the full SDSS and 2dFGRS samples, which contain galaxies that reside in higher density environments. The best-fit values of α for subsamples of the void and wall galaxy samples split by density are also very similar, with the exception of the highest density sample, which exhibits a shallower faint-end slope. This result suggests that the faint-end slope is not strongly dependent

on environment, at least up to cluster densities. A steep value of α for the void galaxy LF would suggest that voids were filled with many dwarf galaxies; we find no such evidence down to $M_r = -14.5$.

3. The void galaxy LF is similar in shape to the LFs of galaxies that reside in higher density environments that are blue, have low values of the Sérsic index, and have high $H\alpha$ equivalent widths although the value of M_r^* for the void galaxy LF is fainter by a statistically significant margin. In contrast, the LFs of red, high Sérsic index, and small $H\alpha$ equivalent widths galaxies found in the higher density environments differ significantly in both shape (flatter faint-end slope than void galaxies) and magnitude scale (brighter M_r^*). This is further evidence that the galaxies in voids are primarily late-type galaxies that are, on average, fainter than those found at higher density.

4. Theoretically, we attribute the ≈ 1 mag shift in M^* between the LFs of the void and wall galaxies to be caused by the shift of the mass function in underdense regions, consistent with the prediction from extended Press-Schechter theory (Goldberg et al. 2005). Semianalytic models also predict that void galaxies should be fainter than wall galaxies (Benson et al. 2003a), consistent with the LFs seen here.

Recent analysis of the LF of the 2dFGRS (Croton et al. 2005) agrees with our results from the SDSS. Thus, the two largest redshift surveys available reach similar conclusions on the void galaxy LF and void galaxy population.

The completed SDSS will cover a wider angle and we will be able to map the distribution of very nearby voids without need of other surveys. It will then be possible to measure the LF of

void galaxies over a wide range of M_r values from one sample alone. We estimate that the final sample will contain roughly 2×10^4 void galaxies among 10^3 large voids (as many unique voids as we currently have void galaxies), which will be large enough that the void galaxy sample itself can be split as a function of color, morphology, star formation rate, and myriad other parameters to further investigate the form of the LF.

Funding for the creation and distribution of the SDSS Archive has been provided by the Alfred P. Sloan Foundation, the participating institutions, the National Aeronautics and Space Administration, the National Science Foundation, the US Department of Energy, the Japanese Monbukagakusho, and the Max Planck Society. The SDSS (<http://www.sdss.org>) is managed by the Astrophysical Research Consortium (ARC) for the participating institutions. The participating institutions are the University of Chicago, Fermilab, the Institute for Advanced Study, the Japan Participation Group, the Johns Hopkins University, the Korean Scientist Group, Los Alamos National Laboratory, the Max-Planck-Institute for Astronomy (MPIA), the Max-Planck-Institut für Astrophysik (MPA), New Mexico State University, University of Pittsburgh, Princeton University, the United States Naval Observatory, and the University of Washington. M. S. V. acknowledges support from NSF grant AST 00-71201 and the John Templeton Foundation. We thank Peder Norberg, Michael Blanton, and David Goldberg for useful conversations. We thank the referee for helpful suggestions that improved this paper.

REFERENCES

- Abazajian, K., et al. 2003, *AJ*, 126, 2081
 ———. 2004, *AJ*, 128, 502
 Balogh, M. L., Baldry, I. K., Nichol, R., Miller, C., Bower, R., & Glazebrook, K. 2004, *ApJ*, 615, L101
 Benson, A. J., Frenk, C. S., Baugh, C. M., Cole, S., & Lacey, C. G. 2003b, *MNRAS*, 343, 679
 Benson, A. J., Hoyle, F., Torres, F., & Vogeley, M. S. 2003a, *MNRAS*, 340, 160
 Berlind, A. A., & Weinberg, D. H. 2002, *ApJ*, 575, 587
 Bingelli, B. 1989, in *Large-Scale Structure and Motions in the Universe*, ed. M. Mezzetti (Dordrecht: Kluwer), 47
 Blanton, M. R., Lin, H., Lupton, R. H., Maley, F. M., Young, N., Zehavi, I., & Loveday, J. 2003a, *AJ*, 125, 2276
 Blanton, M. R., Lupton, R. H., Schlegel, D. J., & Strauss, M. A. 2005, *ApJ*, submitted (astro-ph/0410164)
 Blanton, M. R., et al. 2001, *AJ*, 121, 2358
 ———. 2003b, *AJ*, 125, 2348
 ———. 2003c, *ApJ*, 594, 186
 Bond, J. R., Cole, S., Efstathiou, G., & Kaiser, N. 1991, *ApJ*, 379, 440
 Bromley, B. C., Press, W. H., Lin, H., & Kirshner, R. P. 1998, *ApJ*, 505, 25
 Colless, M. M. 1989, *MNRAS*, 237, 799
 Croton, D. J., et al. 2005, *MNRAS*, 356, 1155
 da Costa, L. N., et al. 1998, *AJ*, 116, 1
 Dekel, A., & Silk, J. 1986, *ApJ*, 303, 39
 de Lapparent, V. 2003, *A&A*, 408, 845
 de Propris, R., et al. 2003, *MNRAS*, 342, 725
 Dressler, A. 1978, *ApJ*, 223, 765
 ———. 1980, *ApJ*, 236, 351
 Efstathiou, G., Ellis, R. S., & Peterson, B. S. 1988, *MNRAS*, 232, 431
 Eisenstein, D. J., et al. 2001, *AJ*, 122, 2267
 Falco, E. E., et al. 1999, *PASP*, 111, 438
 Folkes, S., et al. 1999, *MNRAS*, 308, 459
 Fukugita, M., Ichikawa, T., Gunn, J. E., Doi, M., Shimasaku, K., & Schneider, D. P. 1996, *AJ*, 111, 1748
 Gaidos, E. J. 1997, *AJ*, 113, 117
 Garilli, B. M., Maccagni, D., & Andreon, S. 1999, *A&A*, 342, 408
 Geller, M. J., & Huchra, J. P. 1989, *Science*, 246, 897
 Goldberg, D. M., Jones, T. D., Hoyle, F., Rojas, R.R., Vogeley, M. S., & Blanton, M. R. 2005, *ApJ*, in press (astro-ph/0406527)
 Gómez, P. L., et al. 2003, *ApJ*, 584, 210
 Goto, T., et al. 2002, *PASJ*, 54, 515
 ———. 2003, *PASJ*, 55, 757
 Gottlöber, S., Lokas, E. L., Klypin, A., & Hoffman, Y. 2003, *MNRAS*, 344, 715
 Grogin, N. A., & Geller, M. J. 1999, *AJ*, 118, 2561
 Gunn, J. E., et al. 1998, *AJ*, 116, 3040
 Hoffman, Y., Silk, J., & Wyse, R. F. G. 1992, *ApJ*, 388, L13
 Hogg, D. W., Finkbeiner, D. P., Schlegel, D. J., & Gunn, J. E. 2001, *AJ*, 122, 2129
 Hogg, D. W., et al. 2002, *AJ*, 124, 646
 ———. 2003, *ApJ*, 585, L5
 Hoyle, F., & Vogeley, M. S. 2002, *ApJ*, 566, 641
 ———. 2004, *ApJ*, 607, 751
 Huchtmeier, W. K., Hopp, U., & Kuhn, B. 1997, *A&A*, 319, 67
 Hütsi, G., Einasto, J., Tucker, D. L., Saar, E., Einasto, M., Müller, V., Heinämäki, P., & Allam, S. S. 2003, *A&A*, submitted (astro-ph/0212327)
 Kuhn, B., Hopp, U., & Elsässer, H. 1997, *A&A*, 318, 405
 Lewis, I., et al. 2002, *MNRAS*, 334, 673
 Lin, H., Kirshner, R. P., Shectman, S. A., Oemler, A., Tucker, D. L., & Schechter, P. L. 1996, *ApJ*, 464, 60
 Loveday, J., Efstathiou, G., Peterson, B. A., & Maddox, S. J. 1992, *ApJ*, 400, L43
 Lugger, P. M. 1986, *ApJ*, 303, 535
 Lumsden, S. L., Collins, C. A., Nichol, R. C., Eke, V. R., & Guzzo, L. 1997, *MNRAS*, 290, 119
 Lupton, R. H. 1993, *Statistics in Theory and Practice* (Princeton: Princeton Univ. Press)
 Lupton, R. H., Ivezić, Z., Gunn, J. E., Knapp, G., Strauss, M., & Yasuda, N. 2002, *Proc. SPIE*, 4836, 350
 Madgwick, D. S., et al. 2002, *MNRAS*, 333, 133
 Marzke, R. O., Geller, M. J., Huchra, J. P., & Corwin, H. G., Jr. 1994a, *AJ*, 108, 437
 Marzke, R. O., Huchra, J. P., & Geller, M. J. 1994b, *ApJ*, 428, 43
 Mathis, H., & White, S. D. M. 2002, *MNRAS*, 337, 1193
 Mo, H. J., & White, S. D. M. 1996, *MNRAS*, 282, 347
 Moody, J. W., Kirshner, R. P., MacAlpine, G. M., & Gregory, S. A. 1987, *ApJ*, 314, L33
 Nakamura, O., Fukugita, M., Yasuda, N., Loveday, J., Brinkmann, J., Schneider, D. P., Shimasaku, K., & SubbaRao, M. 2003, *AJ*, 125, 1682

- Norberg, P. et al. 2002a, MNRAS, 332, 827
———. 2002b, MNRAS, 336, 907
- Paolillo, M., Andreon, S., Longo, G., Puddu, E., Gal, R. R., Scaramella, R., Djorgovski, G., & de Carvalho, R. 2001, A&A, 367, 59
- Petrosian, V. 1976, ApJ, 209, L1
- Pier, J. R., et al. 2003, AJ, 125, 1559
- Popescu, C., Hopp, U., & Elsässer, H. 1997, A&A, 325, 881
- Postman, M., & Geller, M. J. 1984, ApJ, 281, 95
- Press, W. H., & Schechter, P. 1974, ApJ, 187, 425
- Ratcliffe, A., Shanks, T., Parker, Q. A., & Fong, R. 1998, MNRAS, 293, 197
- Rauzy, S., Adami, C., & Mazure, A. 1998, A&A, 337, 31
- Rojas, R., Vogeley, M. S., Hoyle, F., & Brinkmann, J. 2004, ApJ, 617, 50
———. 2005, ApJ, in press (astro-ph/0409074)
- Schechter, P. 1976, ApJ, 203, 297
- Schmidt, M. 1968, ApJ, 151, 393
- Scranton, R., et al. 2002, ApJ, 579, 48
- Sérsic, J. L. 1968, Atlas de Galaxias Australes (Córdoba: Observatorio Astronómico)
- Sheth, R. K., & Tormen, G. 2002, MNRAS, 329, 61
- Smith, J. A., et al. 2002, AJ, 123, 2121
- Stoughton, C., et al. 2002, AJ, 123, 485
- Strauss, M., et al. 2002, AJ, 124, 1810
- Szomoru, A., van Gorkom, J. H., Gregg, M. D., & Strauss, M. A. 1996, AJ, 111, 2150
- Trentham, N., & Hodgkin, S. 2002, MNRAS, 333, 423
- Trentham, N., & Tully, R. B. 2002, MNRAS, 335, 712
- Valotto, C. A., Nicotra, M. A., Muriel, H., & Lambass, D. G. 1997, ApJ, 479, 90
- Weistrop, D., Hintzen, P., Liu, C., Lowenthal, J., Cheng, K. P., Oliverson, R., Brown, L., & Woodgate, B. 1995, AJ, 109, 981
- York, D. G., et al. 2000, AJ, 120, 1579
- Zucca, E., et al. 1997, A&A, 326, 477